Nanoscale

Accepted Manuscript

This article can be cited before page numbers have been issued, to do this please use: R. Verre, N. Maccaferri, K. Fleischer, M. Svedendahl, N. Odebo Länk, A. Dmitriev, P. Vavassori, I. Shvets and M. Kall, *Nanoscale*, 2016, DOI: 10.1039/C6NR01336H.

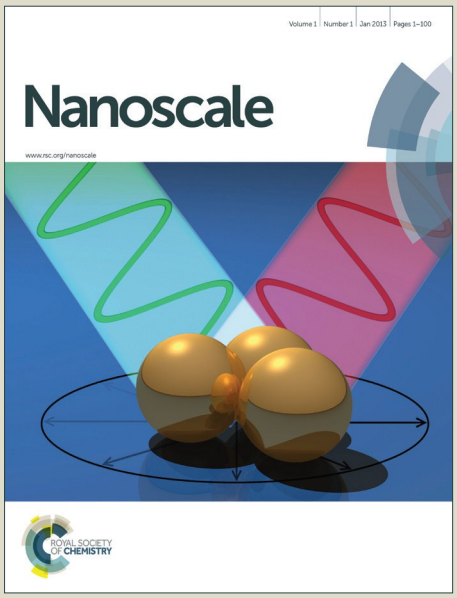

ROYAL SOCIETY OF CHEMISTRY

www.rsc.org/nanoscale

View Article Online
DOI: 10.1039/C6NR01336H

Journal Name

COMMUNICATION

Polarization conversion-based molecular sensing using anisotropic plasmonic metasurfaces

då vi behöver hur många som spela i Abunda med!Received 00th January 20xx,
Accepted 00th January 20xx

DOI: 10.1039/x0xx00000x

www.rsc.org/

R. Verre,[a,] N. Maccaferri,[b] K. Fleischer,[c] M. Svedendahl,[a] N. Odebo Länk,[a] A. Dmitriev,[a] P. Vavassori,[b,d] I.V. Shvets[c] and M. Käll[a]*

Anisotropic media induce changes in the polarization state of transmitted and reflected light. Here we combine this effect with the refractive index sensitivity typical of plasmonic nanoparticles to experimentally demonstrate self-referenced single wavelength refractometric sensing based on polarization conversion. We fabricated anisotropic plasmonic metasurfaces composed of gold dimers and, as a proof of principle, measured the changes in the rotation of light polarization induced by biomolecular adsorption with a surface sensitivity of 0.2ng/cm^2. We demonstrate the possibility of miniaturized sensing and we show that experimental results can be reproduced by analytical theory. Various ways to increase the sensitivity and applicability of the sensing scheme are discussed.

Metallic nanostructures that support localized surface plasmon resonances (LSPRs) have been extensively investigated as transducers for label-free optical biosensing.[1,2] In standard spectroscopic LSPR sensing, the plasmon red shift associated with an increase of the refractive index (RI)in the vicinity of the metal nanostructure are tracked, thereby providing a method to analyze molecular interactions at the nanoscale.[3] The advantages of LSPR sensing rely on the small footprint of the metallic nanostructure, the flexibility in the design geometry of the plasmonic systems, the possibility of integrating them in microfluidic channels[4] and the high local sensitivity due to the strong field enhancement in close proximity to the nanostructure surface.[5, 6]

In a typical LSPR sensing experiment, the intensity of scattered or transmitted light is spectrally analyzed and the plasmon resonance position is tracked versus time. This approach hence requires a spectrometer, the collection of a reference prior to the measurement and good signal stability throughout the entire experiment. Promising simpler routes towards LSPR sensing have utilized complementary properties of light rather than intensity, such as optical phase,[7-9] directionality,[10] polarization or ellipsometric parameters.[11-14].

Recently, an alternative sensing approach based on magneto-optical polarization conversion induced in ferromagnetic plasmonic nanodisks and dimers was presented.[15, 16] The technique displayed high sensitivity to bulk refractive index changes, as well as to adsorption of thin molecular layers.[15] However, a recent theoretical study predicted that even higher sensitivity could be achieved using a polarization rotation sensing scheme applied to anisotropic gold particles.[17] This approach utilizes the high quality factor effects in gold compared to magnetic materials and it does not require an applied magnetic field. Here we experimentally demonstrate LSPR sensing based on polarization conversion in anisotropic gold nanostructures and show that the technique indeed provides an extremely powerful means for real-time analysis of refractive index changes induced by molecular adsorption.

The concept is presented in Figure 1. Linearly polarized monochromatic light is sent at normal incidence towards a

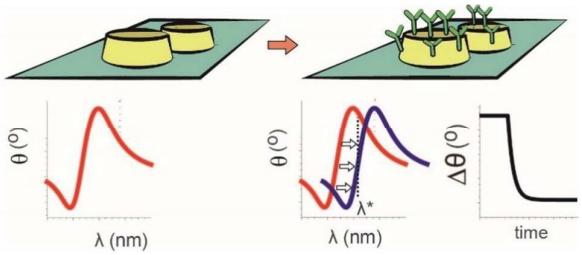

Figure 1. Refractometric sensing using polarization conversion. When a linearly polarized beam is sent at normal incidence towards an anisotropic metasurface, the transmitted beam is elliptically polarized and the polarization axis is rotated with respect to the incident orientation. The polarization rotation and ellipticity can be measured using a polarization sensitive detection scheme and their changes due to environmental changes can be tracked as a function of time at a chosen wavelength λ^*.

[a] *Department of Physics, Chalmers University of Technology, 41296 Göteborg, Sweden*
[b] *CIC nanoGUNE, E-200018 Donostia-San Sebastian, Spain*
[c] *Trinity college of Dublin and Center for Research on Adaptive Nanostructures and Nanodevices (CRANN), Dublin, Ireland*
[d] *IKERBASQUE, Basque Foundation for Science, E-48013 Bilbao, Spain*

View Article Online
DOI: 10.1039/C6NR01336H

metasurface composed of anisotropic plasmonic nanostructures, such as elliptical antennas or dimers. If the polarization plane does not coincide with one of the principal axes of the anisotropic system, the outgoing beam will in general be elliptically polarized with a polarization axis rotated by an angle θ determined by the specific plasmon resonance properties of the system.[18] A polarization-sensitive analysis scheme allows one to measure the change in the polarization state of the transmitted/reflected beam resulting from an LSPR shift and track it in time during molecular binding events.

The technique outlined above has several advantages: the method is self-referenced as it relies only on the polarization state of the light and does not need any previous reference intensity measurement. This means that the technique is stable with respect to sample misalignment, background lighting, spectral shape of the light source and of the detection system, as well as to mechanical drift. Normal incidence illumination allows one to easily implement a microscopic version of this sensing methodology, either in reflection or transmission. Finally, if gold dimers are the constituent anisotropic nanostructures, a very high electric field enhancement in the gap region can be generated, resulting in a high sensitivity to local refractometric changes compared to isolated nanoparticles.[6] In the following, we will illustrate the aforementioned advantages and reach a surface sensitivity of 0.2ng/cm^2.

We first produced gold dimers on a glass substrate using the hole-mask colloidal lithography technique,[19] which allows for the production of large uniform areas composed of identically oriented anisotropic nanoparticles covering the surface in a short-range ordered fashion. The method is cost effective and high throughput and therefore interesting for large-scale applications. After fabrication (see Supplementary Information (SI) for details) the substrate is decorated by high quality Au dimers, as shown in the scanning electron microscopy (SEM) image in Figure 2a. Each particle in the dimer has a height of ~40 nm, an in-plane diameter of ~100 nm and a gap distance of~15 nm, which ensures a strong near-field coupling along the dimer axis and a large field enhancement in the gap.

The anisotropic response of the metasurface was first verified by polarized transmission spectroscopy using normal incidence illumination. As expected, two in-plane resonances corresponding to dipolar plasmon oscillations along (long wavelength resonance) and perpendicular (short wavelength resonance) to the dimer axis were found, as shown in Figure 2b. We also performed Finite Difference Time Domain (FDTD, Lumerical, Canada) simulations, which confirmed the strong field enhancement in the gap region (Figure 2c, see Figure S2 for calculated extinction spectra).

Figure 2d schematically illustrates the polarization sensitive measurements. The sample was illuminated with normally incident light polarized 45° with respect to the dimer axis, in order to maximize the rotation signal, and the transmitted polarization state wasquantified using a photo-elastic modulator (PEM) analyzer setup.[20] Using a lock-in detection scheme, both the polarization ellipticity and rotation can be measured as they are related to the first and second harmonic of the modulation frequency induced by

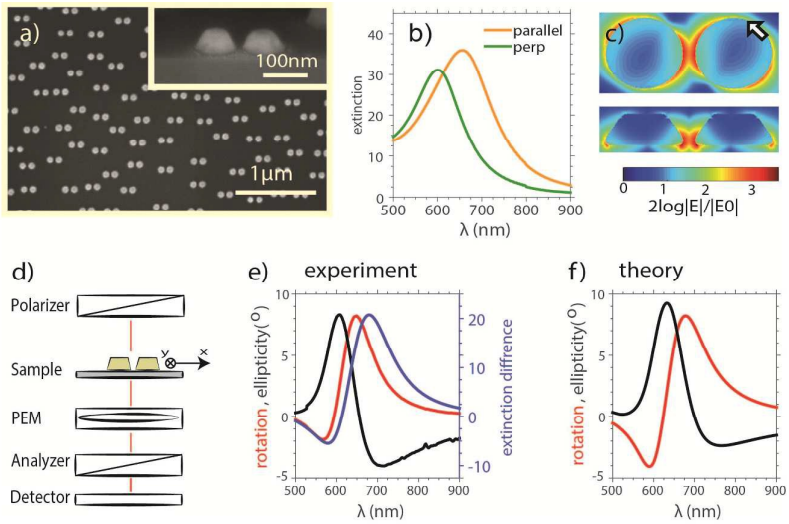

Figure 2. Polarization rotation using an anisotropic metasurface. (a) SEM of the anisotropic metasurface produced. Au dimers cover the glass surface. In the inset a high magnification tilted view is shown. (b) Optical anisotropy measured in extinction for light polarized parallel (orange) and perpendicular (green) to the dimer axis. (c) The simulated near field intensity for the same gold dimer at λ = 650nm. Both top view at the center of the nanoparticle (top) and side view along the dimer axis (bottom) are shown. The arrow indicates the polarization direction of the incoming light (45° from the dimer long-axis). (d) Sketch of the polarization sensitive setup. (e) Experimentally measured polarization rotation (red curve) and ellipticity (black). The rotation spectrum is essentially proportional to the difference in extinction spectra between the two principal directions (blue line). (f) Simulated rotation and ellipticity calculated using the transfer matrix formalism.

View Article Online
DOI: 10.1039/C6NR01336H

the PEM, respectively.[21-22] The technique, also referred to as reflectance anisotropy spectroscopy, has been extensively used in surface analysis, for example to study sub-monolayer adsorbate structures and surface reconstructions.[23-25] However, very few studies have been performed on plasmonic samples.[26-29] The measured rotation shows a negative peak at short wavelengths, at around 590 nm, and a positive and more intense peak(as high as 8°) at around 670 nm (red curve in Figure 2e).To understand the origin of the measured spectral features, we utilized an effective medium approach, as outlined in the SI. In the limit of an optically thin layer thickness d, the polarization state of the light transmitted through the metasurface can be approximated as

$$\theta + i\xi = \frac{\pi d}{\lambda} \frac{i\,(\varepsilon_{L,x} - \varepsilon_{L,y})}{1+n_s}, \qquad (1)$$

where $\varepsilon_{L,j}$ is the effective dielectric function of the metasurface along the j in-plane direction, λ is the wavelength and n_s is the refractive index of the substrate. Equation (1) essentially states that the rotation θ (ellipticity ξ) is proportional to the anisotropy in the imaginary (real) parts of the metasurface dielectric function and to its thickness. If the particles are small and close enough to disregard diffuse scattering, the extinction is $A_j = c/\lambda Im(\varepsilon_{L,j})$. One thus expects the rotation to be proportional to the difference in extinction between the two principal directions.[26] We verify that this is effectively the case in Figure 2e (compare red and blue lines).

In order to gain more quantitative information, we also developed a theory based on a transfer matrix formalism and coupled dipoles.[30-33] First, we computed the effective polarizability of each dimer, taking into account their retarded dipolar interactions [34], and then calculated the effective anisotropic layer dielectric function of the metamaterial using Maxwell-Garnett theory using the experimental dimer density as extracted from SEM images. Finally, using a transfer matrix approach, the rotation was calculated from the complex transmission coefficients (see SI for additional details). The calculations of Figure 2f reproduce the experimental results extremely well. We also experimentally studied the rotation for different dimer dimensions and verified that similar features can be easily tuned through the visible to near-infrared range by changing the nanoparticle geometries (see SI Figure S3-S4). The simulations indicate that the measured rotation angle of 8°can be more than doubled by increasing the spectral separation of the two in-plane resonances or by engineering the geometry of the single disks composing the dimers. Also, we theoretically analyzed in Figure S6 the rotation sensitivity to changes in surrounding media and found that it can also be improved by changing the parameters of the constituent dimer particles.

We now turn to demonstrate how the aforementioned polarization effects can be used for sensing. An increase in the refractive index surrounding the particles will induce a red shift and an increase in the amplitude of the LSPRs. However, this spectral change will be slightly different for the transverse and longitudinal plasmons supported by the dimers, which means that the layer

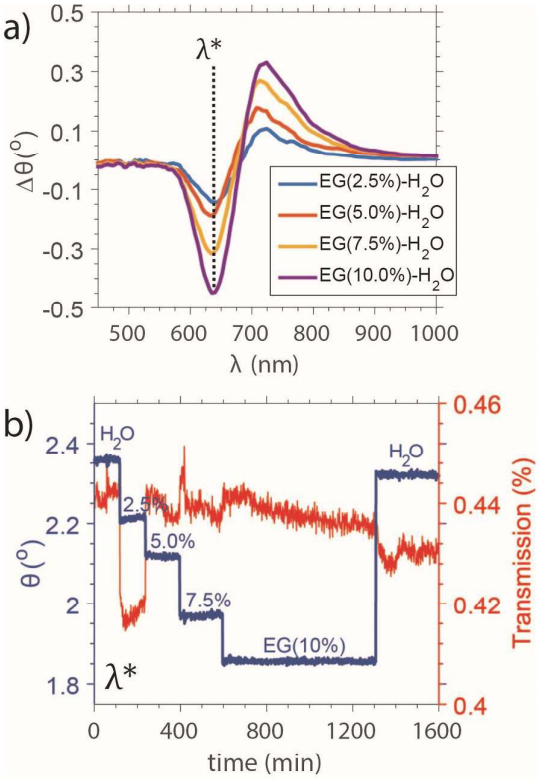

Figure 3. Bulk refractometric sensing using an anisotropic metasurface. (a) Differential polarization rotation spectra for different concentrations of ethylene glycolin water compared to pure water. (b) Comparison between sensing performed using the polarization rotation methodology and simple transmission measurements at the optimum wavelength λ^*. Note the much improved noise level for the rotation measurement.

dielectric anisotropy, and therefore the rotation (see Eq. 1), will change as a function of refractive index. One can thus perform label free refractometric sensing by tracking the spectral change in the polarization rotation, or by simply tracking the rotation at a fixed optimized wavelengthλ^*.

We will first demonstrate, as a proof of principle, this methodology by changing the bulk RI surrounding the particles from n = 1.33 (water) to 1.34. The experiment was done by mixing water with different concentrations of ethylene glycol (EG). In Figure 3a, we plot the change in rotation spectra,$\Delta\theta(\lambda)$, induced by different EG concentrations compared to pure water. The maximum changes are seen to take place at around λ^* = 638nm, which is in between the two in-plane resonance wavelengths (see SI Figure S5 for raw spectra). We then performed transient measurements at λ^* = 638nm by continuously changing the bulk RI and monitoring the rotation in real time to demonstrate the advantage of the polarization-based sensing scheme compared to standard transient transmission measurements, which is defined as the intensity changes (I_{DC}) at the detector divided by the reference signal without nanostructures. The rotation in the current experiment is

View Article Online
DOI: 10.1039/C6NR01336H

measured by dividing the alternating signal at the detector induced by the PEM modulation by the same I_{DC}signal used for the transmission measurements. This provides a way to directly compare the two measurement techniques. While very clear and consistent changes can be observed in the rotation during RI changes, the transmission measurements are obviously too noisy to be convincing. By linear fitting of the rotation, we calculated a bulk sensitivity of 390°±25°/RIU for the particular metasurface under investigation. By optimization of the lock-in sensitivity, which can be done by a slight rotation of the first polarizer, a base noise of 0.0006° was measured using an integration time of 1 sec., which implies that changes in bulk RI as small as 10^{-6} can be detected.

As shown in Fig. 4a, we also verified that the technique can be used for tracking proteinadsorption. Biotylinated bovine serum albumin (bBSA), with a concentration of 100 µg/mL and diluted in a phosphate buffer solution (~0.01M), was first adsorbed on the metasurface and, after rinsing, neutravidin (NA, molecular weight ~60kDa), which couples to biotin, was injected in the same flow cell. Real-time measurements were performed with different NA concentrations and the induced changes in rotation during adsorption were tracked. We observed a saturated change in rotation of ~1°, which is around 800 times larger than the base line noise using a 1 sec. integration time. The saturated signal corresponds to a monolayer of NA on the dimers, or about 400 NA molecules per dimer and 150ng/cm^2 total surface area (assuming ~55% surface coverage obtained through random sequential adsorption.[35 36 37] The base-line noise then gives a detection limit of 0.2ng/cm^2, corresponding to ~0.05 ag or 0.5 NA molecules per dimer, which is one order of magnitude better than what was reported for Ni nanodisks.[15] This is not surprising as the rotation (9°) we achieve in the present experiment is an order of magnitude larger than what can be typically induced by pure magneto-optical rotation. Furthermore, our surface sensitivity is similar to what has been obtained using the most sensitive standard LSPR colorimetric sensing schemes,[38] but the data is here measured at single wavelength and without the need of any fitting procedure. It is likely that state of the art submicro-radiant polarimeter resolution would provide a substantial additional sensitivity improvement.

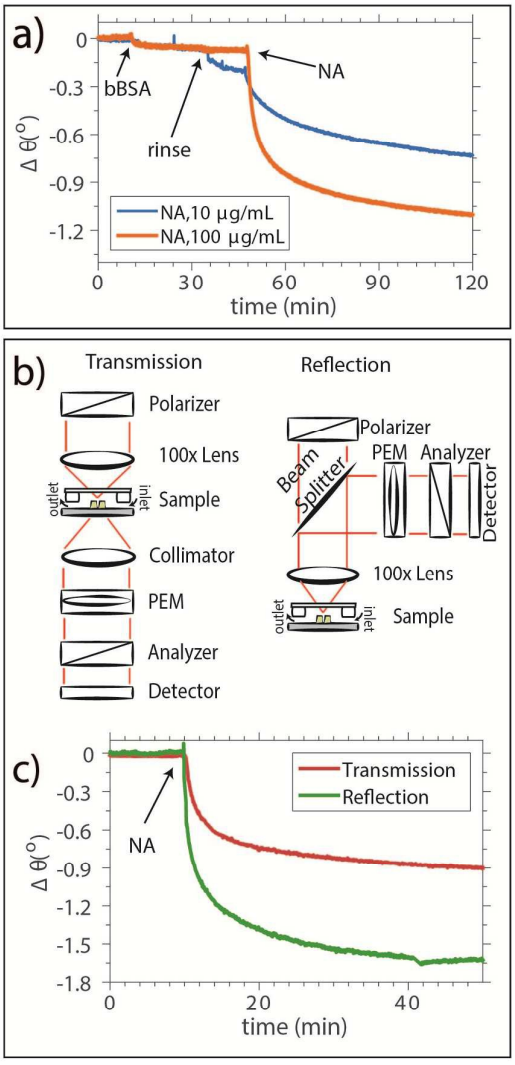

Figure 4. (a) Real time molecular sensing using polarization rotation analysis for two different NA concentrations.(b) Sketch of the micro rotation measurement setups. (c) Real time NA adsorption monitoring using the microscope setups and for an illumination area of ~100x100um^{2}performed in transmission and reflection.

Rather than trying to further optimize the system for ultimate performance, we now turn to the question of miniaturization. This is a key aspect of multiplexed sensing, for example based on multi-channel microfluidics. As sketched in Figure 4b, a 100X long working distance air objective was placed before the sample and, using an aperture, a reduced area of the order 100x100 µm^{2}could be selected. The rotation induced by NA adsorption (a concentration of 100 µg/mL was used) could then be tracked both in transmission and reflection(see Figure 4c, red and green lines), which means that the technique can be easily implemented using both upright and inverted microscopes.

Interestingly, the rotation observed in reflection is approximately twice that in transmission. As previously discussed, the signal is inversely proportional to the overall light intensity I_{DC}. As glass was used as a substrate, the isotropic background in reflection is smaller than the one measured in transmission, which explains the observed different signal amplitudes. Also, the rotation values can be increased by engineering the plasmonic properties of the dimers. For example, in this study a Cr adhesion layer was used, which is known to broaden the resonances[39] and decrease the plasmonic sensitivity. We also theoretically analyzed in Figure S6 the sensitivity $\Delta\theta$/RI and found that it can also be improved by simply changing the parameters of the constituent dimer particles.

For the system and the technique presented here it would also clearly be possible to define a figure of merit, which would essentially be an estimate of the visibility of the peak shifts for bulk changes of the RI of the medium. However, to analyze the performance of the system for biosensing, one should also consider the spatial confinement of the field. For example, while planar surface plasmon resonance sensors exhibit much larger figure of merit for bulk RI sensing compared to LSPR, the two methodologies yield similar resonance shifts upon molecular adsorption due to the better overlap between the near-fields and the molecules in the case of LSPR sensing. For this reason, we rather consider the change in the observable (rotation in the present case) and compare it to the baseline noise to estimate the sensitivity of the system during molecular adsorption.

View Article Online
DOI: 10.1039/C6NR01336H

In conclusion, we have demonstrated a polarization-based LSPR sensing scheme as an alternative to conventional spectroscopic refractive index sensing methods. An anisotropic metamaterial based on plasmonic gold dimers was used as a transducer of molecular interactions in conjunction with a lock-in based detection of polarization rotation. The measurement is self-referenced, surface sensitive and adsorption measurements of molecular species can be easily performed. We demonstrated that the methodology can be adapted to upright (reflection) and an inverted (transmission) microscopes, which indicates that the method is compatible with microfluidics. We demonstrated a bulk refractive index sensitivity of the order 10^{-6} and a molecular adsorption sensitivity of the order 0.2ng/cm^2. However, the sensitivity can most likely be much further improved by precise optimization of the nanostructures and further development of the measurement and analysis methodologies.

Acknowledgements

We would like to thank A.Dahlin and T. Antosiewicz for stimulating discussions. This work was funded by the Knut and Alice Wallenberg Foundation and the Swedish Foundation for Strategic Research. N.M. and P. V. acknowledge support from Basque Government under the Project n. PI2015-1-19 and from MINECO under the Project n. FIS2015-64519-R. N.M. acknowledges support from the Pre-doctoral Program of the Basque Government through the Grant. n. PRE_2015-2-0113 and from the Pre-doctoral Mobility Program of the Basque Government under the grant n. EP2015-1-44. K.F. and I.V.S acknowledge funding by Science Foundation Ireland, grant 06/IN.1/I91.

Notes and references

1. Anker, J. N.; Hall, W. P.; Lyandres, O.; Shah, N. C.; Zhao, J.; Van Duyne, R. P. *Nat Mater* **2008,** 7, (6), 442-453.
2. Stewart, M. E.; Anderton, C. R.; Thompson, L. B.; Maria, J.; Gray, S. K.; Rogers, J. A.; Nuzzo, R. G. *Chemical Reviews* **2008,** 108, (2), 494-521.
3. Cui, Y.; Wei, Q.; Park, H.; Lieber, C. M. *Science* **2001,** 293, (5533), 1289-1292.
4. Aćimović, S. S.; Ortega, M. A.; Sanz, V.; Berthelot, J.; Garcia-Cordero, J. L.; Renger, J.; Maerkl, S. J.; Kreuzer, M. P.; Quidant, R. *Nano Lett.* **2014,** 14, (5), 2636-2641.
5. Zijlstra, P.; Paulo, P. M. R.; Orrit, M. *Nat Nano* **2012,** 7, (6), 379-382.
6. Aćimović, S. S.; Kreuzer, M. P.; González, M. U.; Quidant, R. *ACS Nano* **2009,** 3, (5), 1231-1237.
7. Svedendahl, M.; Verre, R.; Kall, M. *Light Sci Appl* **2014,** 3, e220.
8. Toudert, J.; Wang, X.; Tallet, C.; Barois, P.; Aradian, A.; Ponsinet, V. *ACS Photonics* **2015,** 2, (10), 1443-1450.
9. Lodewijks, K.; Van Roy, W.; Borghs, G.; Lagae, L.; Van Dorpe, P. *Nano Lett.* **2012,** 12, (3), 1655-1659.
10. Wersäll, M.; Verre, R.; Svedendahl, M.; Johansson, P.; Käll, M.; Shegai, T. *J. Phys. Chem. C* **2014,** 118, 21075-21080.
11. Piliarik, M.; Šípová, H.; Kvasnička, P.; Galler, N.; Krenn, J. R.; Homola, J. *Opt. Express* **2012,** 20, (1), 672-680.
12. Moirangthem, R. S.; Chang, Y.-C.; Hsu, S.-H.; Wei, P.-K. *Biosensors and Bioelectronics* **2010,** 25, (12), 2633-2638.
13. Arwin, H.; Poksinski, M.; Johansen, K. *Appl. Opt.* **2004,** 43, (15), 3028-3036.
14. Kravets, V. G.; Schedin, F.; Kabashin, A. V.; Grigorenko, A. N. *Opt. Lett.* **2010,** 35, (7), 956-958.
15. Maccaferri, N.; Gregorczyk, K. E.; de Oliveira, T. V.; Kataja, M.; van Dijken, S.; Pirzadeh, Z.; Dmitriev, A.; Åkerman, J.; Knez, M.; Vavassori, P. *Nature Communications* **2015,** 6, 6150.
16. Zubritskaya, I.; Lodewijks, K.; Maccaferri, N.; Mekonnen, A.; Dumas, R. K.; Åkerman, J.; Vavassori, P.; Dmitriev, A. *Nano Lett.* **2015,** 15, (5), 3204-3211.
17. Liu, S.-D.; Qi, X.; Zhai, W.-C.; Chen, Z.-H.; Wang, W.-J.; Han, J.-B. *Nanoscale* **2015,** 7, (47), 20171-20179.
18. Hect, B.; Zajac, A., *Optics*. Addison-Wesley: 1974.
19. Fredriksson, H.; Alaverdyan, Y.; Dmitriev, A.; Langhammer, C.; Sutherland, D. S.; Zäch, M.; Kasemo, B. *Adv. Mat.* **2007,** 19, 4297-4302.
20. Aspnes, D. E.; Studna, A. A. *Phys. Rev. Lett.* **1985,** 54, (17), 1956-1959.
21. Weightman, P.; Martin, D. S.; Cole, R. J.; Farrell, T. *Reports on Progress in Physics* **2005,** 68, (6), 1251.
22. Vavassori, P. *Appl. Phys. Lett.* **2000,** 77, (11), 1605-1607.
23. Fleischer, K.; Verre, R.; Mauit, O.; Sofin, R. G. S.; Farrell, L.; Byrne, C.; Smith, C. M.; McGilp, J. F.; Shvets, I. V. *Physical Review B* **2014,** 89, (19), 195118.
24. Hogan, C.; Ferraro, E.; McAlinden, N.; McGilp, J. F. *Phys. Rev. Lett.* **2013,** 111, (8), 087401.
25. Fleischer, K.; Chandola, S.; Esser, N.; Richter, W.; McGilp, J. F.; Schmidt, W. G.; Wang, S.; Lu, W.; Bernholc, J. *Applied Surface Science* **2004,** 234, (1–4), 302-306.
26. Verre, R.; Fleischer, K.; Sofin, R. G. S.; McAlinden, N.; McGilp, J. F.; Shvets, I. V. *Physical Review B* **2011,** 83, (12), 125432.
27. Verre, R.; Fleischer, K.; McGilp, J. F.; Fox, D.; Behan, G.; Zhang, H.; Shvets, I. V. *Nanotechnology* **2012,** 23, (3), 035606.
28. Verre, R.; Fleischer, K.; Ualibek, O.; Shvets, I. V. *Appl. Phys. Lett.* **2012,** 100, (3), 031102.
29. Ualibek, O.; Verre, R.; Bulfin, B.; Usov, V.; Fleischer, K.; McGilp, J. F.; Shvets, I. V. *Nanoscale* **2013,** 5, (11), 4923-4930.
30. Verre, R.; Modreanu, M.; Ualibek, O.; Fox, D.; Fleischer, K.; Smith, C.; Zhang, H.; Pemble, M.; McGilp, J. F.; Shvets, I. V. *Physical Review B* **2013,** 87, (23), 235428.
31. Maccaferri, N.; González-Díaz, J. B.; Bonetti, S.; Berger, A.; Kataja, M.; van Dijken, S.; Nogués, J.; Bonanni, V.; Pirzadeh, Z.; Dmitriev, A. *Opt. Express* **2013,** 21, (8), 9875-9889.
32. Schubert, M. *Physical Review B* **1996,** 53, (8), 4265-4274.
33. Schubert, M.; Tiwald, T. E.; Woollam, J. A. *Appl. Opt.* **1999,** 38, (1), 177-187.
34. Boris, K.; Andrei, M.; Vladimir, Z.; Nikolai, K. *Nanotechnology* **2006,** 17, (5), 1437.
35. Adamczyk, Z.; Siwek, B.; Zembala, M.; Belouschek, P. *Advances in Colloid and Interface Science* **1994,** 48, 151-280.
36. Rosano, C.; Arosio, P.; Bolognesi, M. *Biomolecular Engineering* **1999,** 16, (1–4), 5-12.
37. Huang, N.-P.; Vörös, J.; De Paul, S. M.; Textor, M.; Spencer, N. D. *Langmuir* **2002,** 18, (1), 220-230.
38. Dahlin, A. B.; Tegenfeldt, J. O.; Höök, F. *Analytical Chemistry* **2006,** 78, (13), 4416-4423.
39. Aouani, H.; Wenger, J.; Gérard, D.; Rigneault, H.; Devaux, E.; Ebbesen, T. W.; Mahdavi, F.; Xu, T.; Blair, S. *ACS Nano* **2009,** 3, (7), 2043-2048.